GSA Data Repository 2016006

# Magma reservoir response to transient recharge events: the case of Santorini volcano

**Wim Degruyter[1,2], Christian Huber[1], Olivier Bachmann[2], Kari Cooper[3], and Adam Kent[4]**

[1]*School of Earth and Atmospheric Sciences, Georgia Institute of Technology, 311 Ferst Drive, Atlanta, GA 30332, USA*

[2]*Institute of Geochemistry and Petrology, ETH Zurich, Clausiusstrasse 25, CH-8092 Zurich, Switzerland*

[3]*Department of Earth and Planetary Sciences, University of California, Davis, One Shield Avenue, Davis, California 95616, USA*

[4]*College of Earth, Ocean and Atmospheric Sciences, 104 Ocean Administration, Oregon State University, Corvallis, Oregon 97331, USA*

## SUPPLEMENTARY METHODS

### Response of thermal models to pulsating inflow

In this section, we explore the response of diffusion to a pulsating source term. Consider the one-dimensional diffusion equation:

$$\left\{\frac{\partial}{\partial t} - D\frac{\partial^2}{\partial x^2}\right\}\psi(x,t) = \rho(x,t),$$

with $t$ time, $x$ position, D the (constant) diffusivity, $\psi$ the quantity that is diffusing (e.g., heat), and $\rho$ a source term. For the sake of argument, we solve this equation on a one-

dimensional rod with finite length *L*. We thereby assume no-flux (von Neumann) boundary conditions at both ends of the rod, i.e. *x*=0 and *x*=*L*. At the center of the rod (*x*=L/2), we inject heat at a certain rate, starting at time *t*=0, giving

$$\rho(x,t) = \theta(t)f(t)\delta(x' - L/2),$$

with $\theta$ the Heaviside function (to turn on the source at *t*=0), f the time-varying part of the source term, and $\delta$ the kronecker delta positioning the source at the center of the pipe. Under these conditions the diffusion equation has an analytical solution of the form

$$\psi(x,t) = \int_0^t dt' \int_0^L dx' G(x,t|x',t')\rho(x,\square),$$

with *G* the Green's function for von Neumann boundary conditions given by

$$G(x,t|x',t') = \theta(t-t')\frac{2}{L}$$

$$\mathrm{x}\left\{\frac{1}{2} + \sum_{n=1}^{\infty} \cos\left(\frac{n\pi x'}{L}\right)\cos\left(\frac{n\pi x}{L}\right)\exp\left(-D\left(\frac{n\pi}{L}\right)^2(t-t')\right)\right\}.$$

If we define the function g as follows

$$g(x,t) = \frac{1}{2} + \sum_{n=1}^{\infty} \cos\left(\frac{n\pi}{2}\right)\cos\left(\frac{n\pi x}{L}\right)\exp\left(-D\left(\frac{n\pi}{L}\right)^2 t\right),$$

we can now simply write the solution of the diffusion equation as the convolution of the time-varying part of the source term *f* and the function *g* with respect to time,

$$\psi(x,t) = (f * g)(t).$$

We now define the time-varying part of the source term as rectangular pulses,

$$f(t) = \sum_{n=0}^{\infty}\left[\theta\left(t - n\tau_p\right) - \theta\left(t - n\tau_p - \tau_d\right)\right]$$

where $\theta$ is again the Heaviside function, $\tau_p$ is the period between pulses, and $\tau_d$ is the duration of a pulse (Fig. S1). If the time-averaged injection rate is given by $\bar{\omega}$, than the

injection rate of a pulse is defined by $\omega_p = \bar{\omega}\frac{\tau_p}{\tau_d}$. For diffusion models of this type (like thermal models for magma emplacement), the behavior can be either diffusion-limited, i.e. the transfer of $\psi$ is limited by the rate at which it can be diffused, or it is injection-limited, i.e. the transfer is limited by the amount that is injected at the source. This bifurcation in behavior can be quantified by defining the characteristic time scale of diffusion $\tau_{diff} = \frac{L^2}{D}$. If $\tau_{diff} \gg \tau_d$ then we are in the diffusion-limited regime (Fig. DR1a). In this case, the sharp pulses are smoothed out by diffusion and at the edge of the pipe the source term is seen as a continuous inflow. Else, if $\tau_{diff} \ll \tau_d$ then we are in the injection-limited regime (Fig. DR1b). In this case, diffusion is so fast that at the edge of the pipe, the injection rate is nearly exactly the same as at the source location. We quantify this by randomly sampling a range of (i) $D$ between $10^{-1}$ and 10 $m^2/s$, (ii) $\tau_p$ between $10^{-1}$ and 10 s, and (iii) $\tau_d/\tau_p$ between $10^{-2}$ and 1. We set $\bar{\omega} = 1$. We use the cross-correlation between the heat flow rate at the source and the edge of the pipe as a measure for determining which process (injection or diffusion) is limiting. We find that this is completely determined by the ratio of $\tau_{diff}/\tau_d$ (Fig. DR2). If this ratio is below 1 we are in the injection-limited regime and above 100 we are in the diffusion-limited regime. These results illustrate the behavior expected from thermal models exposed to episodic recharge (Schopa and Annen, 2013). In the case that the recharge duration is shorter than the conduction timescale of the crust (diffusion-limited), the crust will respond as if to a continuous recharge having the inflow-rate averaged over one period, i.e. the long-term average inflow rate. Only in the case where the recharge duration is longer than the conduction timescale (injection-limited), the cooling of the crust will respond to the recharge injection rate (as opposed to the long-term average rate). The

critical injection rate, for which a chamber with mobile magma can be formed, will then be the same as for a continuous injection of the same magnitude (Annen, 2009; Schopa and Annen, 2013).

**Summary of the thermo-mechanical magma chamber model**

The thermo-mechanical chamber model is based on the following main assumptions:

(i) The magma chamber is assumed to be spherical. The actual shape of magma chamber is likely not to be a perfect sphere, but this assumption will only impact the absolute values of the calculations, and not the relative trends or feedbacks between the different processes. For the heat loss only a factor of ~3 in the timing of cooling is expected (Caricchi et al., 2014) and for a sill-shaped chamber the stress is expected to accumulate near the edges of the chamber (Karlstrom et al., 2012), as opposed to be distributed more uniformly for a sphere.

(ii) The magma is homogeneous across the chamber.

(iii) The phases (melt, crystals and possibly gas) are in equilibrium.

(iv) The magma chamber loses heat into a colder crustal shell that responds visco-elastically to pressure changes in the magma chamber. The crustal shell can be seen as the crystal-rich mush near the magma chamber that continues into the crust in the far-field.

(v) An eruption starts when the magma is mobile (<50% crystals) and the pressure in the magma chamber reaches a critical overpressure (40 MPa). An eruption ends when the pressure returns to the lithostatic pressure.

(vi) Episodic recharge is modeled as rectangular pulses, for which the pulse duration and rate are varied such that the long-term average inflow rate is constant and equal to 0.001 $km^3$/yr (Fig. DR3).

These assumptions allow us to model the thermo-mechanical evolution of a magma chamber by solving the conservation of (total) mass,

$$\frac{dM}{dt} = \dot{M}_{in} - \dot{M}_{out},$$

the conservation of total (=dissolved + exsolved) water,

$$\frac{dM^w}{dt} = \dot{M}^w_{in} - \dot{M}^w_{out},$$

and the conservation of enthalpy

$$\frac{dH}{dt} = \dot{H}_{in} - \dot{H}_{out},$$

with $M$ the total mass, $M^w$ the mass of water and $H$ the total enthalpy. The terms with indexes *in* and *out* contain the sources and sinks for these variables. The detailed derivation and solution method are described by (Degruyter and Huber, 2014).

**Definition of timescales**

- Recharge injection timescale, $\tau_{inflow} = \frac{V_0}{\dot{V}_{in}}$.
- Cooling timescale, $\tau_{cool} = \frac{V_0^{2/3}}{\kappa}$.
- Viscous relaxation timescale, $\tau_{relax} = \frac{\eta_r}{(\Delta P)_c}$.

## References


Annen, C., 2009, From plutons to magma chambers: Thermal constraints on the accumulation of eruptible silicic magma in the upper crust: Earth and Planetary Science Letters, v. 284, no. 3-4, p. 409-416.

Caricchi, L., Simpson, G., and Schaltegger, U., 2014, Zircons reveal magma fluxes in the Earth/'s crust: Nature, v. 511, no. 7510, p. 457-461.

Degruyter, W., and Huber, C., 2014, A model for eruption frequency of upper crustal silicic magma chambers: Earth and Planetary Science Letters, v. 403, no. 0, p. 117-130.

Druitt, T. H., Costa, F., Deloule, E., Dungan, M., and Scaillet, B., 2012, Decadal to monthly timescales of magma transfer and reservoir growth at a caldera volcano: Nature, v. 482, no. 7383, p. 77-80.

Karlstrom, L., Rudolph, M. L., and Manga, M., 2012, Caldera size modulated by the yield stress within a crystal-rich magma reservoir: Nature Geosci, v. 5, no. 6, p. 402-405.

Parks, M. M., Biggs, J., England, P., Mather, T. A., Nomikou, P., Palamartchouk, K., Papanikolaou, X., Paradissis, D., Parsons, B., Pyle, D. M., Raptakis, C., and Zacharis, V., 2012, Evolution of Santorini Volcano dominated by episodic and rapid fluxes of melt from depth: Nature Geoscience, v. 5, no. 10, p. 749-754.

Schopa, A., and Annen, C., 2013, The effects of magma flux variations on the formation and lifetime of large silicic magma chambers: Journal of Geophysical Research-Solid Earth, v. 118, no. 3, p. 926-942.

## SUPPLEMENTARY FIGURES

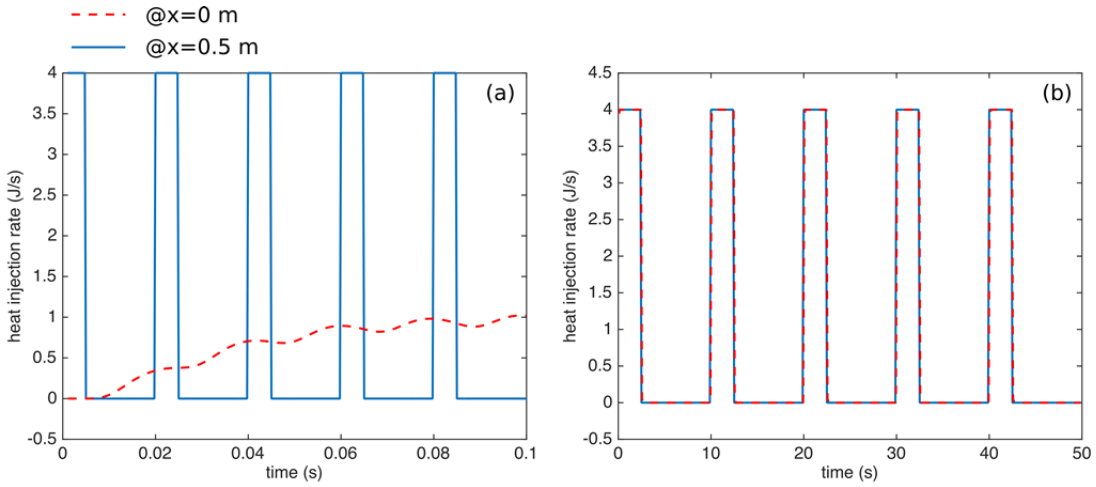


Figure DR1: Solution of the heat injection rate in a one-dimensional pipe for L=1 m and D= 1 $m^2/s$ for different source terms. The characteristic timescale for diffusion is and $\tau_{diff} = 0.25$ s. The solution shows the heat injection rate at the source point x=L/2=0.5 m and at one of the edges of the pipe, x=0 m. (a) Diffusion-limited case: $\tau_p = 0.02$ s, $\tau_d = 0.005$ s. (b) Injection-limited case: $\tau_p = 10$ s, $\tau_d = 2.5$ s. In both (a) and (b), we have $\bar{\omega} = 1$ J/s resulting in $\omega_p = 4$ J/s.

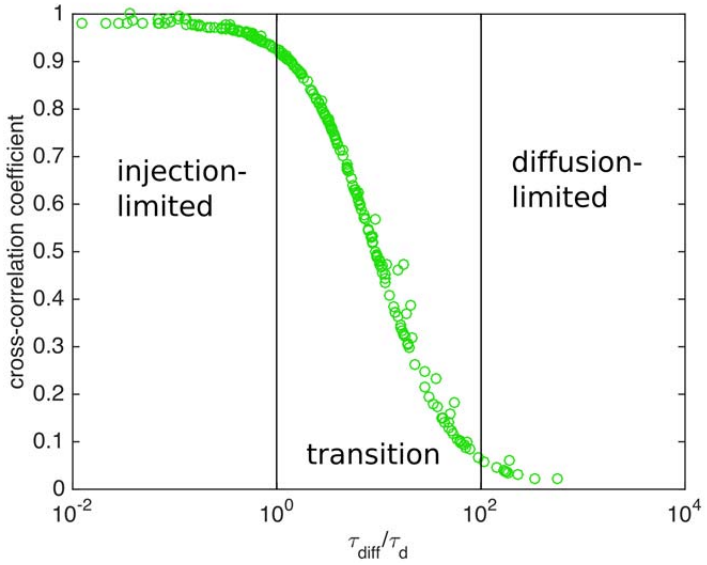


Figure DR2: Cross-correlation between the heat flow at the source position and the edge of the pipe. When the value is close to 1, the heat flux signals at the center and ends of the rod are nearly identical in shape (not necessary in magnitude), which determines the injection-limited regime. As the correlation coefficient decreases to values close to 0, the heat flux at the ends of the rod carries little information about the heat source at the center of the rod, which characterizes the diffusion-limited regime.

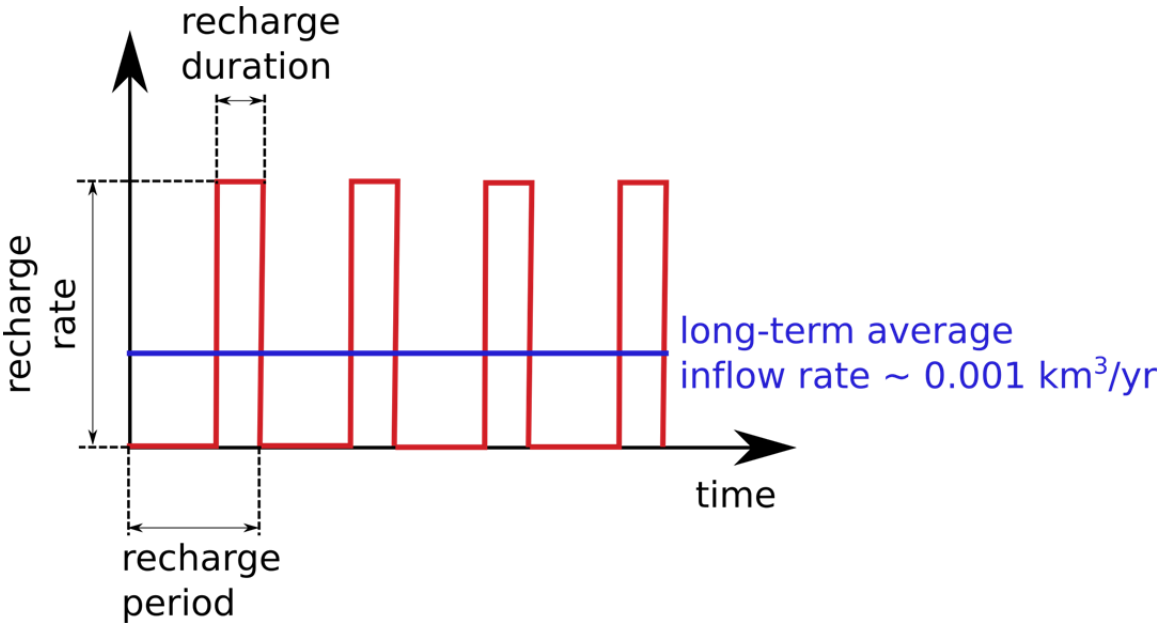


Figure DR3: Schematic representation of the modeled recharge events. The recharge duration and rate are modeled such that the long-term average inflow rate remains constant.

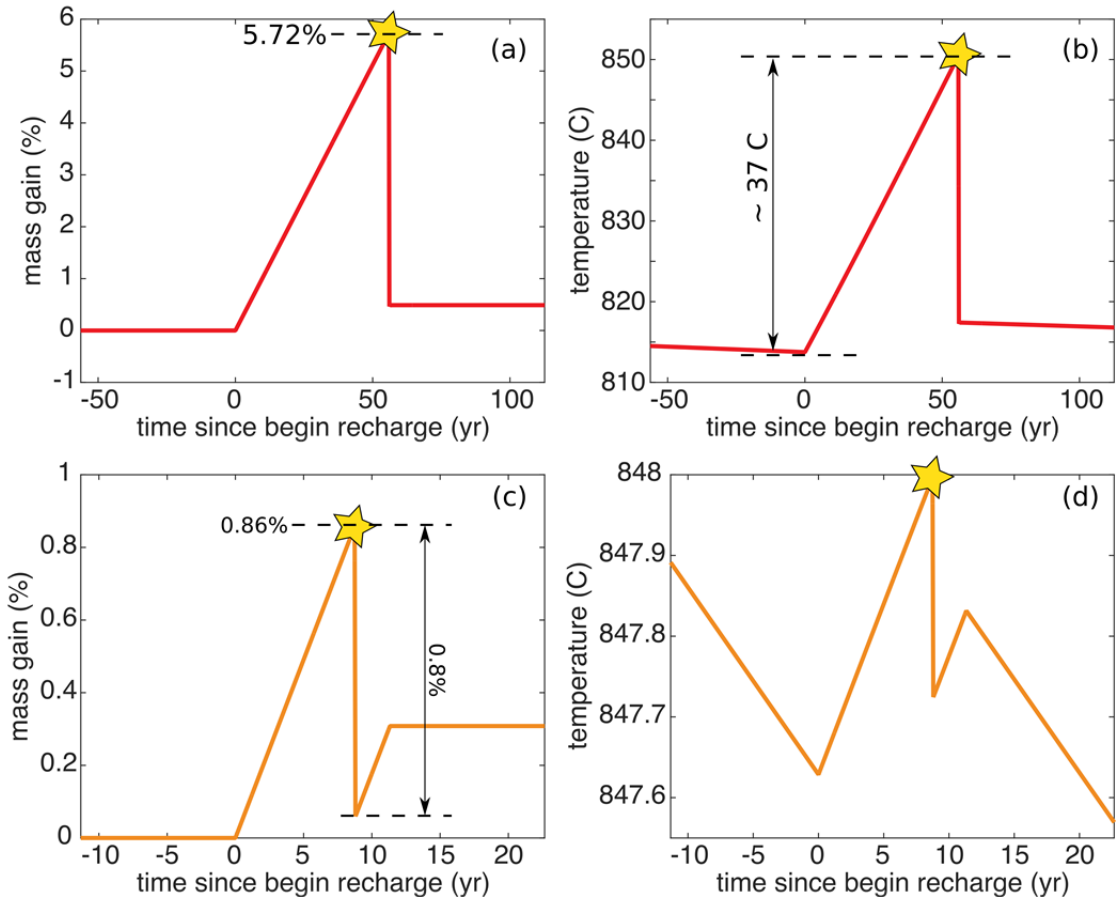


Figure DR4: Mass and temperature evolution for the eruption scenarios depicted in Fig. 1. The yellow star represents the onset of the eruption. (a) Increase in mass in the magma chamber and (b) temperature evolution for the recharge scenario shown in Fig. 1a (long-term average inflow rate of $10^{-3}$ $km^3$/yr, initial chamber volume of 50 $km^3$, recharge duration 56 yr, recharge rate $5x10^{-2}$ $km^3$/yr, saturated magma). The increase in mass of magma stored in the chamber (~6%) and its average temperature increase (~ 40 °C) at the time of the eruption are both consistent with chemical mass balance considerations and reheating inferred by (Druitt et al., 2012). (c) and (d) show the evolution of the same variables in the context of the recharge scenario depicted in Fig. 1b for the Nea Kameni eruptions (long-term average inflow rate of $10^{-3}$ $km^3$/yr, initial chamber volume of 10 $km^3$, recharge duration 11 yr, recharge rate $10^{-2}$ $km^3$/yr, no exsolved volatiles present in

the magma). We find that the recharge that triggered the eruption accounts for less than 1% of the total mass of magma in the chamber, in agreement with estimates from the proportion of the mafic enclaves in the erupted products (Parks et al., 2012). Additionally, the mass erupted is 0.8% of the chamber mass, which is 0.08 $km^3$ DRE, which corresponds to the estimates of erupted volumes (Parks et al., 2012). Note that the temperature increase in panel (d) is almost negligible compared to panel (b). This indicates again the very different thermal evolution of a 2-phase chamber versus a 3-phase chamber.